



## Fixation strength of four headless compression screws



Adam Hart<sup>a,\*</sup>, Edward J. Harvey<sup>a</sup>, Reza Rabiei<sup>b</sup>, Francois Barthelat<sup>b</sup>, Paul A. Martineau<sup>a</sup>

<sup>a</sup> Division of Orthopaedic Surgery, McGill University Health Centre, Montreal, Quebec, Canada

<sup>b</sup> Department of Mechanical Engineering, McGill University, Montreal, Quebec, Canada

### ARTICLE INFO

#### Article history:

Received 22 December 2015

Revised 25 April 2016

Accepted 19 June 2016

#### Keywords:

Biomechanical

Headless compression screw

Pull apart

Four point bending

Scaphoid fracture

### ABSTRACT

To promote a quicker return to function, an increasing number of patients are treated with headless screws for acute displaced and even non-displaced scaphoid fractures. Therefore, it is imperative to understand and optimize the biomechanical characteristics of different implants to support the demands of early mobilization. The objective of this study was to evaluate the biomechanical *fixation strength* of 4 headless compression screws under distracting and bending forces. The Acutrak Standard, Acutrak Mini, Synthes 3.0, and Herbert-Whipple screws were tested using a polyurethane foam scaphoid fracture model. Implants were inserted into the foam blocks across a linear osteotomy. Custom fixtures applied pull-apart and four-point bending forces until implant failure. Pull-apart testing was performed in three different foam densities in order to simulate osteoporotic, osteopenic, and normal bone. The peak pull-apart forces varied significantly between implants and were achieved by (from greatest to least): the Acutrak Standard, Synthes 3.0, Acutrak Mini, and Herbert-Whipple screws. The fully threaded screws (Acutrak) failed at their proximal threads while the shanked screw (Synthes and Herbert Whipple) failed at their distal threads. Similarly, the screws most resistant to bending were (from greatest to least): the Acutrak Standard, Acutrak Mini, Herbert-Whipple, and Synthes. Although the amount of force required for pull-apart failure increased with each increasing simulated bone density (a doubling in density required triple the amount of pull apart force), the mode and sequence of failure was the same. Overall, the fully threaded, conical design of the Acutrak screws demonstrated superior fixation against pull-apart and bending forces than the shanked designs of the Synthes and Herbert-Whipple. We also found a strong relationship between simulated bone density and pull-apart force.

© 2016 IPREM. Published by Elsevier Ltd. All rights reserved.

### 1. Introduction

Traditionally, nondisplaced and minimally displaced scaphoid fractures have been considered stable and were treated conservatively with cast immobilization. Although this approach achieves healing rates ranging from 90% to 100% [1,2], there is a trend in orthopaedic practice towards early internal fixation of these injuries in order to avoid prolonged immobilization and expedite return to work [3] and sport [4]. This is especially true for the young and active patient in whom these injuries are most prevalent [5]. Prospective randomized trials [6,7] have compared cast immobilization to percutaneous fixation with a headless compression screw (HCS); demonstrating a significantly quicker time to union and return to work in the surgical group notwithstanding

the occurrence of some surgical complications. Subsequent meta-analysis [8] confirmed improved standardized functional outcomes in patients treated with surgery in lieu of casting.

As more patients are offered surgical fixation of these injuries, and thus growing emphasis on early mobilization, the post-operative fixation of the implant to provide absolute stability [9,10] is of increasing importance. Numerous studies have examined the interfragmentary compression of HCSs [11–13]; however, little is known about the strength of current implants to withstand the deforming forces within a mobilizing carpus. Furthermore, the few studies that describe biomechanical testing through pull-apart [14–16], bending [17,18], and cyclical loading [19] mostly involve a comparison to the original Herbert screw rather than current, widely used implants.

The primary objective of this study was to evaluate the biomechanical *fixation strength* of 4 popular, commercially available HCSs under the forces the scaphoid is subjected to with early motion: distraction and bending [20]. These two modes of failure were tested in a polyurethane foam scaphoid model by measuring the pull-apart and four-point bending forces respectively. As a secondary objective, we tested the pull-apart force of each implant

\* Corresponding author. McGill University Health Centre, Division of Orthopaedic Surgery, 1650 Cedar Avenue, A5-175.1, Montreal, Quebec, H3G 1A4. Fax: +1 514 934 8394.

E-mail addresses: [adam.hart@mail.mcgill.ca](mailto:adam.hart@mail.mcgill.ca) (A. Hart), [ejharvey@videotron.ca](mailto:ejharvey@videotron.ca) (E.J. Harvey), [reza.rabiei@mail.mcgill.ca](mailto:reza.rabiei@mail.mcgill.ca) (R. Rabiei), [francois.barthelat@mcgill.ca](mailto:francois.barthelat@mcgill.ca) (F. Barthelat), [paul.martineau@mail.mcgill.ca](mailto:paul.martineau@mail.mcgill.ca) (P.A. Martineau).

in 3 different foam densities – simulating osteoporotic, osteopenic, and normal bone. Our null hypothesis was that there would be no difference in fixation strength between implants and that the pull-apart force would increase proportionately with denser bone.

## 2. Materials and methods

### 2.1. Implants

Four commercially available HCSs were tested (Fig. 1). All screws were chosen to have similar length (24–25 mm) in order to control for bone purchase. The *Acutrak Standard* (Acumed, Hillsboro, OR) is a highly polished titanium, conically shaped, self-tapping, fully threaded, cannulated screw with a variable thread pitch spanning the entire screw. It has a distal outer-diameter (DOD) of 3.3 mm, and proximal outer-diameter (POD) of 4.4 mm. The *Acutrak Mini* (Acumed, Hillsboro, OR) is a scaled-down version of the *Acutrak-Standard* with DOD and POD of 2.8 mm and 3.5 mm respectively. The *Synthes 3.0 mm HCS* (DePuy Synthes, West Chester, PA) is a cannulated 316 L stainless steel, self-drilling and self-tapping headless screw with DOD and POD of 3.0 mm and 3.5 mm respectively. A smooth shank that allows for pre-compression to be applied during screw insertion separates the distal and proximal threads. Finally, the *Herbert-Whipple HCS* (Zimmer, Warsaw, IN) is a modified version of the original Herbert screw with a slightly larger diameter (2.5 mm) to accommodate cannulation and has self-tapping leading threads. Made of Titanium (Ti-6Al-4V alloy), the DOD and POD are 3.0 mm and 3.85 mm respectively, separated by a smooth 2.5 mm diameter shank between proximal and distal threads.

### 2.2. Scaphoid bone model

Biomechanical stability was studied using a rigid polyurethane foam scaphoid fracture model (1522-1-3, Pacific Research Laboratories, Vashon, WA). In addition to providing consistent interspecimen size, shape, density, and screw purchase, these foams have been specifically validated by the American Society for Testing and Materials as a cancellous bone testing medium for orthopaedic implants [21]. Polyurethane foam has therefore been used extensively for biomechanical evaluation of scaphoid screws [13,15,22–27]. The biomechanical properties of the foam are well

controlled, compress and crush like cancellous bone, and were selected to best approximate scaphoid cancellous bone of a young adult [28,29] – comprising a density of 0.32 g/cc (20 pcf). Pull-apart testing was repeated in 0.24 g/cc (15 pcf) and 0.16 g/cc (10 pcf) to simulate osteopenic and osteoporotic bone respectively [30].

The foam was machined by computer numerical control into 10 mm by 30 mm by 70 mm blocks and a diamond saw created a linear osteotomy at the midpoint. The model simulates a scaphoid waist fracture perpendicular to the long axis of the bone and therefore a best-case scenario for fixation (equal screw purchase on either side of the fracture, no comminution, and fixation perpendicular to the fracture). Each implant under test was inserted into a new fracture specimen (specimens were never re-used) according to the manufacturer guidelines. A drill press was used in lieu of a freehand drill to ensure accurate placement of the implant in the center and perpendicular to the fracture specimen. The implants were buried into the foam block by 2 mm from the surface (as recommended by the implant manufacturers and practiced clinically by the authors), achieving compression between the two fracture fragments. Approximately two screw turns of pre-compression was applied to the Synthes screw using the compression sleeve provided by the manufacturer. A stopper was used to ensure the screws were placed equidistant across the fracture plane.

### 2.3. Pull-apart

A custom fixture (Fig. 2A) separated the two halves of the foam block at a constant speed of 0.05 mm/s while continuously recording the applied force and displacement of the fracture until one end of the implant entirely dislodged from the foam. The displacement was produced by a motorized torque meter (Imada, Northbrook, IL). The mode of failure was recorded for each implant. The experiments were performed using 0.16, 0.24, and 0.32 g/cc foam and repeated 6 times per implant type for a total of 72 tests.

### 2.4. Four-point bending

A custom apparatus (Fig. 2B) applied bending stresses on either side of the simulated fracture plane through a four-point configuration at a rate of 0.01 mm/s while a chronometric camera

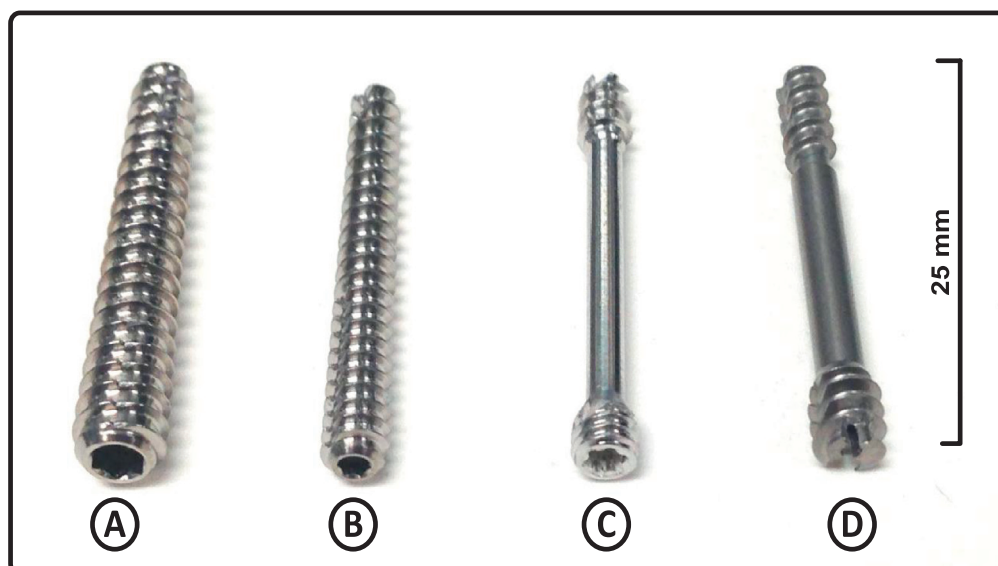


Fig. 1. Four HCSs tested: (a) Acutrak Standard, (b) Acutrak Mini, (c) Synthes 3.0, (d) Herbert-Whipple.

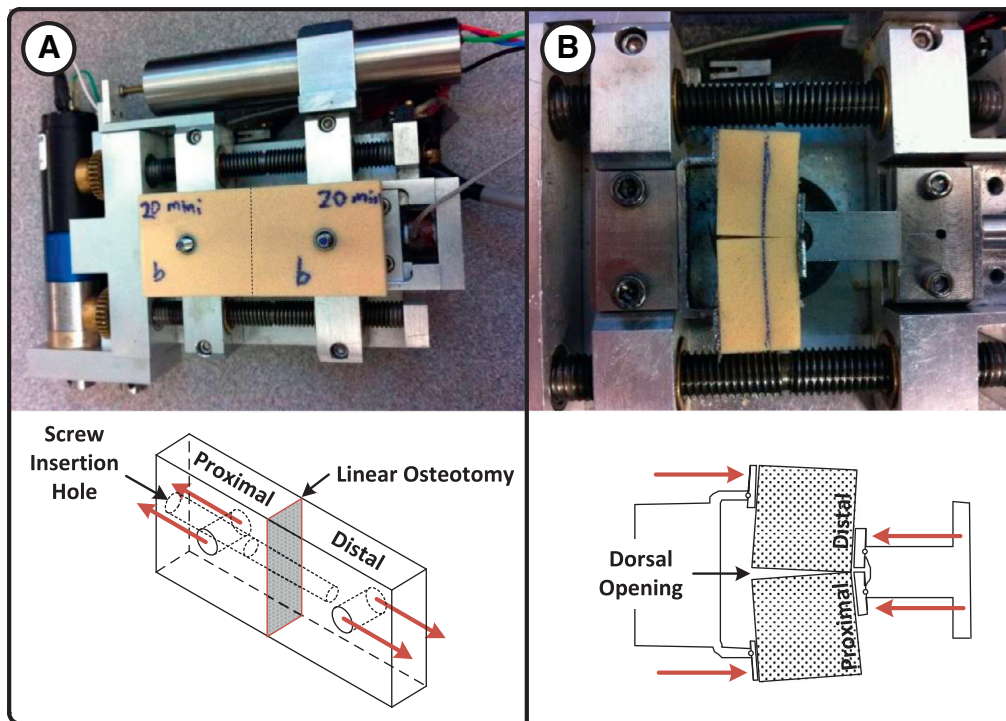


Fig. 2. Experimental setup for (A) pull-apart and (B) 4 point bending testing.

recorded the experiment. Four articulated steel plates were inserted between the legs of the fixture and the sample in order to prevent indentation into the soft polyurethane foam. As the bending increased, the forces created compression on one side of the fracture and separation on the other (crack displacement opening). The images provided accurate measurement ( $\pm 0.01$  mm) of the crack displacement opening and two points of failure were defined: 0.5 mm and 1 mm. The tangent modulus was calculated at both these points using the slope of the force-displacement curve. Stiffness (slope of the force displacement curve in the toe region) was also calculated for each implant. The experiments were performed using 0.32 g/cc foam (simulating normal cancellous bone of a young adult) and repeated 6 times per implant type for a total of 24 tests.

### 2.5. Statistical methods

Pull-apart and four-point bending curves were generated for each implant. Descriptive statistics (mean and standard error) and one-way analysis of variance (ANOVA) were used to analyze the peak pull-apart forces and four-point bending results among the four implants. A significance level (alpha) of 0.05 was used in the statistics software (Matlab, R2009b, Mathworks, Natick, MA).

Preliminary validation of the pull-apart and four-point bending setup provided measurements with standard deviation up to 12% of the mean. In order to have a standard error of less than 5% of the mean, each experiment was repeated six times.

## 3. Results

A *pull-apart profile* (applied force versus fracture displacement) was created for each implant as shown in Fig. 3 for the Acutrak Mini. The six individual trials for each screw were combined into the *composite profiles* shown in Fig. 4 where the performance of each HCS is directly compared across the three foam densities. The lines and error bars represent the mean and standard error respectively. The peak pull-apart forces are summa-

rized in Fig. 5 and were, from greatest to least, achieved by the Acutrak Standard, Synthes 3.0, Acutrak Mini, and Herbert-Whipple screws respectively (in all three foam densities). One-way ANOVA analysis demonstrated a significant difference between each screw ( $P < 0.01$ ) except between the Acutrak Mini and Herbert-Whipple in the osteopenic and normal density foams. The dominant mode of failure was proximal loosening for the Acutrak and Herbert-Whipple screws whereas the Synthes failed at the distal threads.

Four-point bending profiles (applied force versus apparatus displacement) were produced for each implant as exemplified in Fig. 6A for the Synthes HCS where markers "X" and "O" represent the average dorsal crack displacement openings of 0.5 mm and 1 mm respectively. In the toe region, the mean stiffness of each implant was 142 N/mm, 98 N/mm, 85 N/mm, and 102 N/mm for the Acutrak Standard, Acutrak Mini, Synthes 3.0, and Herbert-Whipple screws respectively. One way ANOVA demonstrated a significant difference in stiffness between all implants except the Acutrak Mini and Herbert-Whipple screws ( $P = 0.006$ ). The HCSs most resistant to bending at 0.5 and 1 mm were achieved by, from greatest to least, the Acutrak Standard, Acutrak Mini, Herbert-Whipple, and Synthes (Fig. 6B). The force required to cause crack displacement openings of both 0.5 mm and 1 mm were significantly different amongst all implants ( $P < 0.01$ ) except between the Synthes and Herbert-Whipple screws. Apparent rigidity, defined as the slope of the force-displacement curve is shown in Fig. 6C for both endpoints.

## 4. Discussion

In the present study, 96 polyurethane scaphoid models were used to test the biomechanical fixation strength of 4 commonly used implants. We found that the peak pull-apart forces varied significantly between implants and were achieved by (from greatest to least): the Acutrak Standard, Synthes 3.0, Acutrak Mini, and Herbert-Whipple screws. The fully threaded screws (Acutrak) failed at their proximal threads while the shanked screws (Synthes and Herbert Whipple) failed at their distal threads. The screws most

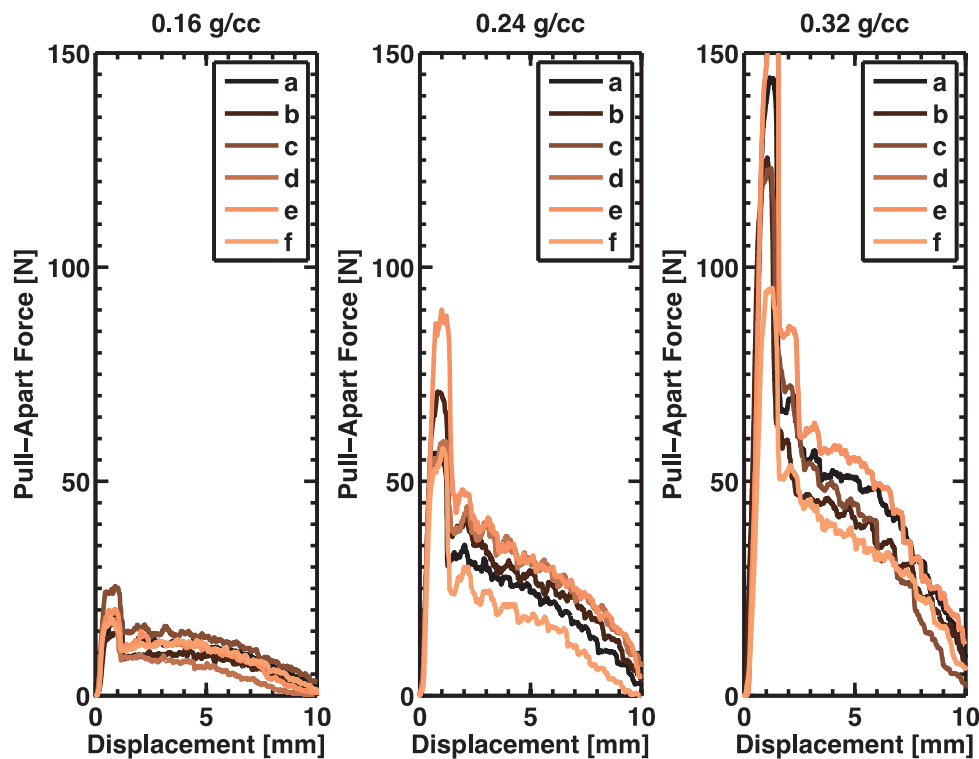


Fig. 3. Pull-apart profile of Acutrak Mini in foam densities of 0.16, 0.24, and 0.32 g/cc where a–f represent the six identical implants tested.

resistant to bending were (from greatest to least): the Acutrak Standard, Acutrak Mini, Herbert-Whipple, and Synthes. Although the amount of force required for pull-apart failure increased with each increasing simulated bone density (a doubling in density required triple the amount of pull apart force), the mode and sequence of failure was the same.

The ability to withstand pull-apart force was significantly better with the Acutrak Standard and Synthes screws, resisting up to three times more force than the other HCSs before failing (Fig. 5). This is in stark contrast to a similar study by Crawford et al. [25] who found the pull-apart force of the Herbert-Whipple almost twice that of the Acutrak Standard. The difference might be explained by the sizable (4.2 mm) gap between their fracture fragments, which undoubtedly discriminates against the fully threaded Acutrak screw. Although there was a statistically significant difference between screws, it should be noted that all four endured over 100 N of pull-apart (in 0.32 g/cc foam), which appears to be adequate for the expected forces within the carpus. Older studies which tested the original Herbert screw found that it had inferior pullout strength in comparison to a 4.0 mm ASIF cancellous screw [14] as well as an Acutrak standard screw [16].

The mode of failure during pull-apart was remarkably different between the shanked and Acutrak screws. Although both have a peak pull-apart force within 1 mm of displacement, the shanked screws demonstrate a ductile failure with a rather flat force-displacement curve whereas the Acutrak screws exhibit brittle failure and quickly loosen beyond 1 mm of displacement (Fig. 4). Intuitively, this may be explained by the conical shape of the Acutrak, which causes disengagement of the threads as the screw backs out whereas compaction of trabecular bone along the non-thread part of the shanked screws may contribute to the ductile behavior. Nevertheless, this loosening only occurs beyond 1 mm of displacement, which is not clinically important because the screw is well beyond the point of failure (the reduction is lost and the bone fragments are no longer well opposed).

The force required to cause failure under four-point bending was significantly higher for the Acutrak screws compared to the shanked screws. The Acutrak, threaded from tip to tip and with larger core diameter, may endow superior interference fitting between fragments under bending forces while shanked screws piston along their smooth, thinner shaft. Nonetheless, increased resistance to bending failure of the Acutrak must be balanced with its larger footprint across the fracture site which may compromise its blood supply and area available for healing [31]. The relative performance amongst screws did not change between 0.5 mm and 1 mm of crack displacement opening; however, only about 30% more force was required; suggesting the implants had begun to loosen. Apparent rigidity, calculated as the slope of the force-displacement curve, confirms there is loosening beyond 0.5 mm of opening resulting in a commensurate loss of rigidity. Again, all four implants withstood applied bending forces greater than 200 N which should be more than sufficient to resist the typical intercarpal forces.

The relative performance of the implants was similar across foam densities; however, it increased dramatically in higher foam density. In general, the strength of solid foams, including trabecular bone and the polyurethane foams used here, are proportional to density [32]. In our experiment, the average pull-apart force jumped by a factor of 3 between densities of 0.16 and 0.32 g/cc. While scaphoid fractures are uncommon in patients with osteopenic or osteoporotic bone, the significant reduction in fixation strength under distraction forces may advise against surgical management in these patients or longer immobilization after fixation with a screw.

Our testing model aimed to simulate the deforming forces exerted on the scaphoid during early mobilization of the wrist following surgery as described by earlier studies. Rainbow et al. [33] studied the *in vivo* kinematics of the intact scaphoid and identified bending forces in extreme loaded extension as unbalanced, leaving the scaphoid and supporting ligaments vulnerable to

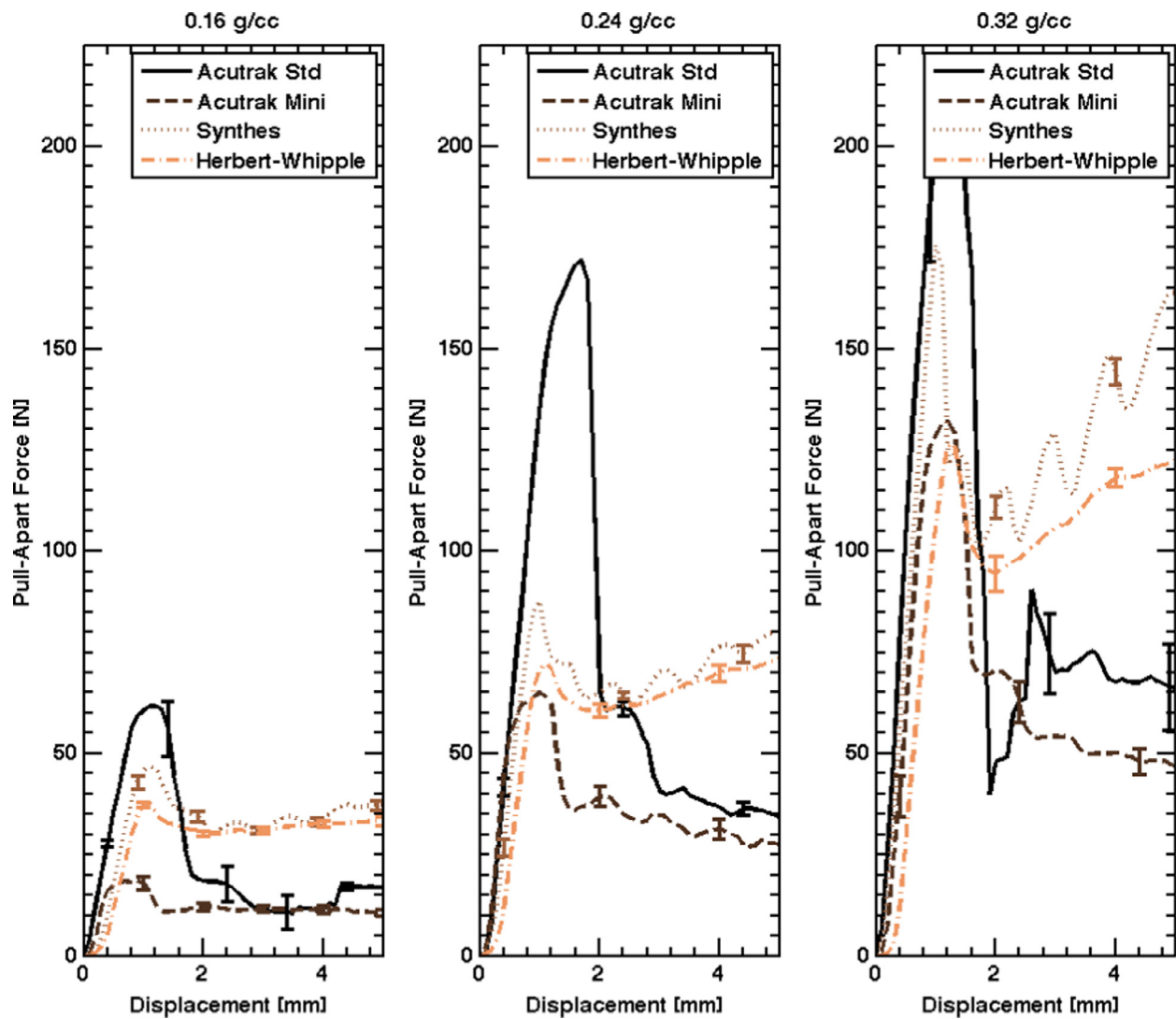


Fig. 4. Combined pull-apart profiles in foam density of 0.16, 0.24, and 0.32 g/cc. Error bars represent the standard error about the mean.

rupture. In a cadaveric study using wrists with loaded tendons, Smith et al. [20] observed the tendency of a scaphoid osteotomy to collapse into a dorsally angulated deformity during wrist movements. The classic “humpback” deformity [34] of a scaphoid non-union also supports these findings. The fixation strength of the scaphoid-implant construct therefore depends on its ability to endure distraction (pull-apart) and bending of the fracture fragments. While cyclical loading, such as that employed by Toby et al. [19], tests both these parameters together, it is difficult to mimic the true dynamic loading that occurs *in vivo* [35]. Furthermore, the authors hypothesize that early bone-implant failures occur from catastrophic loading rather than cyclical fatigue. We therefore opted to test pull-apart and bending separately in a highly reproducible load-to-failure polyurethane foam model so that the behavior of each implant and mode of failure could be studied independently.

How much fixation strength must an implant provide to a newly united scaphoid? A recent study by Varga et al. [36] used finite element modeling to estimate the contact forces on the scaphoid in various functional, unloaded wrist positions. The forces ranged from 0.08 to 25 N and were highest in total extension. Tang et al. [37] studied the contact pressure at the radiocarpal joint using pressure sensitive film in a cadaver model and found an average scaphoid contact pressure of 1.4 MPa on a surface

area of 45–78 mm<sup>2</sup> (63–109 N). A similar study by Rikli et al. [38] performed *in vivo* demonstrated forces in the radial center of the radiocarpal joint of 15–59 N. While these studies provide a ballpark estimate of the forces acting on the newly united scaphoid, additional factors such as the quality of the bone, geometry of the fracture, and activity of the patient must also be considered.

Limitations of this study stem from the challenge of creating a realistic fracture model on which accurate biomechanical testing can be performed. The model used in this study was *ex vivo* in polyurethane foam and did not include soft tissue attachments. Furthermore, the simulated fracture was a simple linear osteotomy perpendicular to the implant, which may misrepresent eccentric screw positioning, the frictional forces between jagged fracture fragments or comminution. Nonetheless, this fracture model has been used extensively in the biomechanical testing literature [13,15,22–27] and obviates the use of cadaveric specimens which are usually of much lower bone density (due to advanced age) and prone to higher inter-specimen variations in terms of shape and mechanical properties [11,39–42]. Our study analyzed fixation strength in pull-apart and bending modes separately; however, the true clinical scenario is most likely a cyclical combination of both forces. Notwithstanding these limitations, the evaluation of implants on the highly reproducible model employed in this study

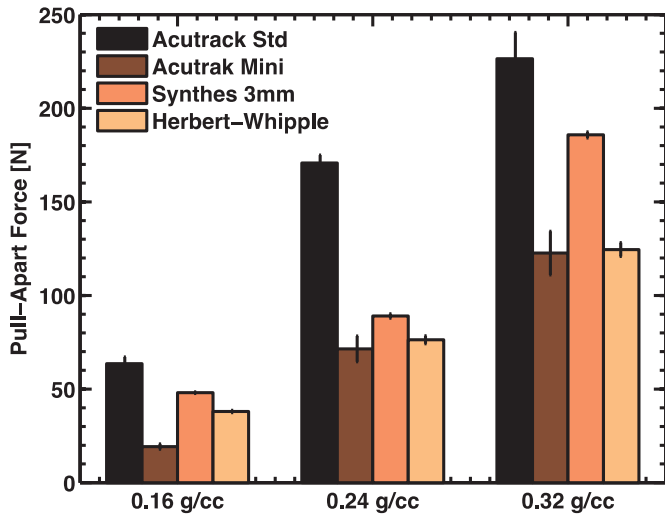


Fig. 5. Bar graph of peak pull-apart force for each HCS in 0.16, 0.24, and 0.32 g/cc foam densities. Error bars represent the standard error about the mean.

provided a comparative platform to test implants with important clinical implications.

Keeping these limitations in mind, the pull-apart and four-point bending profiles generated in this study suggest the following clinical corollaries. The pull-apart force is substantially reduced in osteopenic and osteoporotic bone, warning against fixation in these patients or use of prolonged post-operative immobilization. A crack displacement opening of more than 0.5 mm on post-operative imaging is likely to correlate to implant stripping, significant reduction in construct rigidity, and possible implant failure as demonstrated in this study. Without exact knowledge of the magnitude and mode of forces acting on the healing scaphoid, it is unknown how much fixation strength is necessary to achieve union. Nonetheless, the fully threaded, conical design of the Acutrak has superior fixation strength compared to the shanked designs of the Synthes and Herbert-Whipple, while all four implants provided sufficient fixation for the distraction and bending forces typically expected in a mobilizing scaphoid. The Acutrak Standard had higher pull-apart and resistance to four point bending compared to the Mini; however, it comes at the expense of a larger screw profile which may compromise the healing potential of the bone.

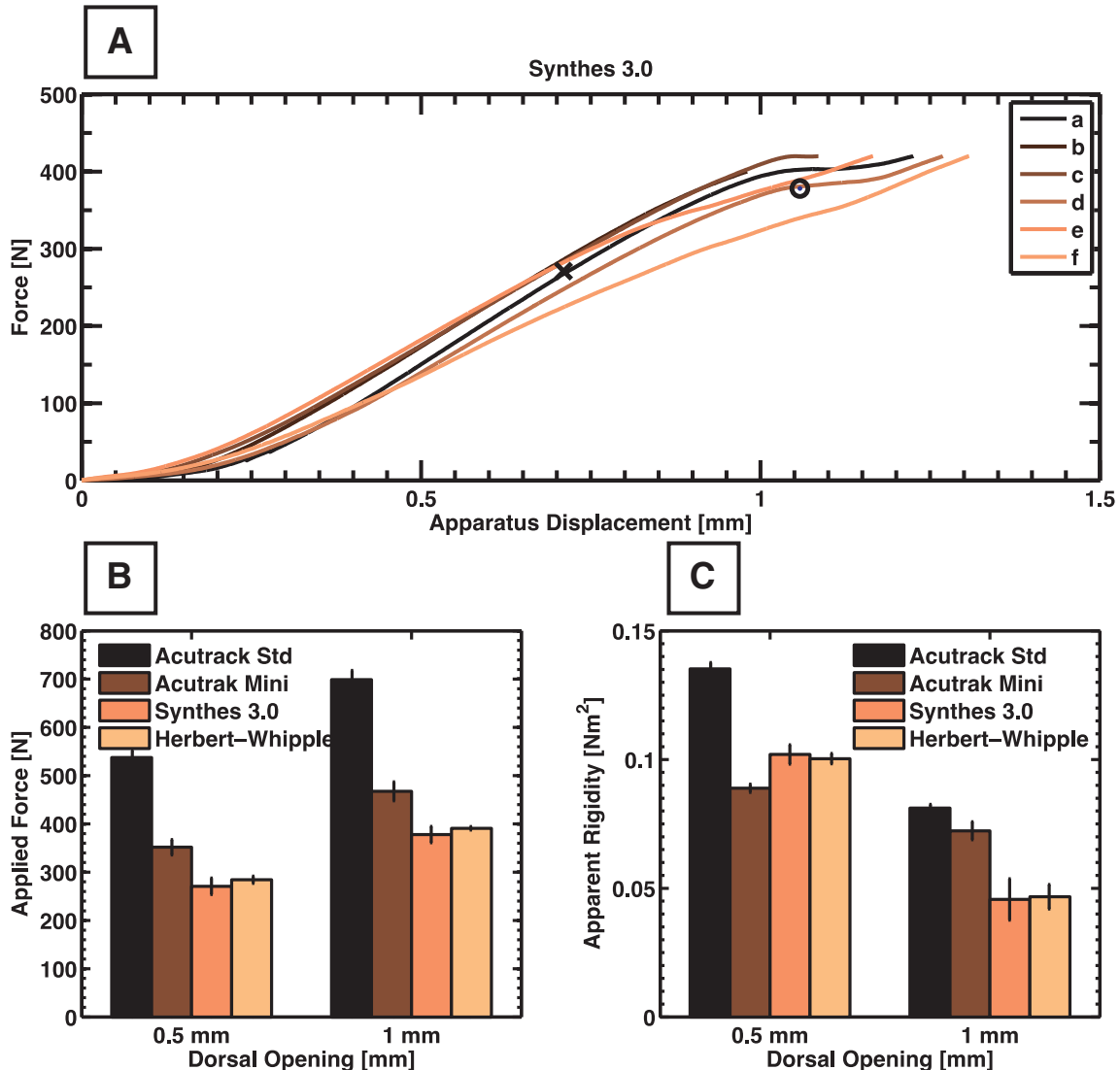


Fig. 6. Four-point bending profile for the Synthes 3.0 HCS (A) where a–f represent the six identical implants tested. Markers X and O represent the average displacement and force required to cause 0.5 mm and 1 mm of crack displacement opening respectively. Bending profiles comparing the applied force (B) and apparent rigidity (C) when the crack displacement opening is 0.5 mm and 1 mm.

## Conflict of interest

All named authors hereby declare that they have no conflicts of interest to disclose.

## Acknowledgment

The specimens and equipment used in this study were funded by a research grant from the [Canadian Institutes of Health Research](#) as well as support from Consultation Semperform Inc.

## References

- [1] Hambidge JE, Desai VV, Schranz PJ, Compson JP, Davis TR, Barton NJ. Acute fractures of the scaphoid. Treatment by cast immobilisation with the wrist in flexion or extension? *J Bone Joint Surg Br Vol* 1999;81:91–2.
- [2] Gellman H, Caputo RJ, Carter V, Aboualfia A, McKay M. Comparison of short and long thumb-spica casts for non-displaced fractures of the carpal scaphoid. *J Bone Joint Surg Am Vol* 1989;71:354–7.
- [3] Fowler JR, Ilyas AM. Headless compression screw fixation of scaphoid fractures. *Hand Clinics* 2010;26:351–61 vi.
- [4] Geissler WB. Arthroscopic management of scaphoid fractures in athletes. *Hand Clinics* 2009;25:359–69.
- [5] Hove LM. Epidemiology of scaphoid fractures in Bergen, Norway. *Scand J Plastic Reconstructive Surg Hand Surg/Nordisk plastikkirurgisk forening [and] Nordisk klubb for handkirurgi* 1999;33:423–6.
- [6] McQueen MM, Gelbke MK, Wakefield A, Will EM, Gaebler C. Percutaneous screw fixation versus conservative treatment for fractures of the waist of the scaphoid: a prospective randomised study. *J Bone Joint Surg Br Vol* 2008;90:66–71.
- [7] Bond CD, Shin AY, McBride MT, Dao KD. Percutaneous screw fixation or cast immobilization for nondisplaced scaphoid fractures. *J Bone Joint Surg Am Vol* 2001;83-A:483–8.
- [8] Buijze GA, Doornberg JN, Ham JS, Ring D, Bhandari M, Poolman RW. Surgical compared with conservative treatment for acute nondisplaced or minimally displaced scaphoid fractures: a systematic review and meta-analysis of randomized controlled trials. *J Bone Joint Surg Am Vol* 2010;92:1534–44.
- [9] Rüedi TP, Murphy WM. *AO principles of fracture management*. Stuttgart; New York; Davos Platz, Switzerland: Thieme; AO Pub; 2000.
- [10] Rajeev Jahagirdar BES. *Principles of fracture healing and disorders of bone union*. Surgery 2009;27:63–9.
- [11] Gruszka DS, Burkhart KJ, Nowak TE, Achenbach T, Rommens PM, Muller LP. The durability of the intrascaphoid compression of headless compression screws: in vitro study. *J Hand Surg* 2012;37:1142–50.
- [12] Pency RA, Richards AM, Belkoff SM, Mentzer K, Andrew Eglseider W. Biomechanical comparison of two headless compression screws for scaphoid fixation. *J Surg Orthop Adv* 2009;18:182–8.
- [13] Hart A, Harvey EJ, Lefebvre LP, Barthelat F, Rabiei R, Martineau PA. Insertion profiles of 4 headless compression screws. *J Hand Surg* 2013;38:1728–34.
- [14] Lange RH, Vanderby Jr, Engber WD, Glad RW, Purnell ML. Biomechanical and histological evaluation of the Herbert screw. *J Orthop Trauma* 1990;4:275–82.
- [15] Baran O, Sagol E, H OX, Sarikanat M, Havitcioglu H. A biomechanical study on preloaded compression eVect on headless screws. *Arch Orthop Trauma Surg* 2009;129:1601–5.
- [16] Wheeler DL, McLoughlin SW. Biomechanical assessment of compression screws. *Clin Orthop Relat Res* 1998:237–45.
- [17] Carter FM 2nd, Zimmerman MC, DiPaola DM, Mackessy RP, Parsons JR. Biomechanical comparison of fixation devices in experimental scaphoid osteotomies. *J Hand Surg* 1991;16:907–12.
- [18] Kaulesar Sukul DM, Johannes EJ, Marti RK, Klopper PJ. Biomechanical measurements on scaphoid bone screws in an experimental model. *J Biomech* 1990;23:1115–21.
- [19] Toby EB, Butler TE, McCormack TJ, Jayaraman G. A comparison of fixation screws for the scaphoid during application of cyclical bending loads. *J Bone Joint Surg Am Vol* 1997;79:1190–7.
- [20] Smith DK, An KN, Cooney WP 3rd, Linscheid RL, Chao EY. Effects of a scaphoid waist osteotomy on carpal kinematics. *J Orthop Res: Official Publ Orthop Res Soc* 1989;7:590–8.
- [21] Standard specification for rigid polyurethane foam for use as a standard material for testing orthopaedic devices and instruments; 2012.
- [22] Adla DN, Kitsis C, Miles AW. Compression forces generated by mini bone screws—a comparative study done on bone model. *Injury* 2005;36:65–70.
- [23] Bailey CA, Kuiper JH, Kelly CP. Biomechanical evaluation of a new composite bioresorbable screw. *J Hand Surg* 2006;31:208–12.
- [24] Brown GA, McCarthy T, Bourgeault CA, Callahan DJ. Mechanical performance of standard and cannulated 4.0-mm cancellous bone screws. *J Orthop Res: Official Publ Orthop Res Soc* 2000;18:307–12.
- [25] Crawford LA, Powell ES, Trail IA. The fixation strength of scaphoid bone screws: an in vitro investigation using polyurethane foam. *J Hand Surg* 2012;37:255–60.
- [26] Hausmann JT, Mayr W, Unger E, Benesch T, Vecsei V, Gabler C. Interfragmentary compression forces of scaphoid screws in a sawbone cylinder model. *Injury* 2007;38:763–8.
- [27] Sugathan HK, Kilpatrick M, Joyce TJ, Harrison JW. A biomechanical study on variation of compressive force along the Acutrak 2 screw. *Injury* 2012;43:205–8.
- [28] Lee SB, Kim HJ, Chun JM, Lee CS, Kim SY, Kim PT, et al. Osseous microarchitecture of the scaphoid: Cadaveric study of regional variations and clinical implications. *Clin Anat* 2012;25:203–11.
- [29] Qu G, von Schroeder HP. Trabecular microstructure at the human scaphoid nonunion. *J Hand Surg* 2008;33:650–5.
- [30] Patel PS, Shepherd DE, Hukins DW. Compressive properties of commercially available polyurethane foams as mechanical models for osteoporotic human cancellous bone. *BMC Musculoskelet Disord* 2008;9:137.
- [31] Hart A, Mansuri A, Harvey EJ, Martineau PA. Central versus eccentric internal fixation of acute scaphoid fractures. *J Hand Surg* 2013;38:66–71.
- [32] Gibson LJ, Ashby MF. *Cellular solids: structure and properties*. 2nd ed. Cambridge; New York: Cambridge University Press; 1997.
- [33] Rainbow MJ, Kamal RN, Leventhal E, Akelman E, Moore DC, Wolfe SW, et al. In vivo kinematics of the scaphoid, lunate, capitate, and third metacarpal in extreme wrist flexion and extension. *J Hand Surg* 2013;38:278–88.
- [34] Cohen MS, Jupiter JB, Fallahi K, Shukla SK. Scaphoid waist nonunion with humpback deformity treated without structural bone graft. *J Hand Surg* 2013;38:701–5.
- [35] Gunal I. A comparison of fixation screws for the scaphoid during application of cyclical bending loads. *J Bone Joint Surg Am Vol* 1998;80:1245.
- [36] Varga P, Schefzig P, Unger E, Mayr W, Zysset PK, Erhart J. Finite element based estimation of contact areas and pressures of the human scaphoid in various functional positions of the hand. *J Biomech* 2013;46:984–90.
- [37] Tang P, Gauvin J, Muriuki M, Pfaeffle JH, Imbriglia JE, Goitz RJ. Comparison of the "contact biomechanics" of the intact and proximal row carpectomy wrist. *J Hand Surg* 2009;34:660–70.
- [38] Rikli DA, Honigmann P, Babst R, Cristalli A, Morlock MM, Mittlmeier T. Intra-articular pressure measurement in the radiocarpal joint using a novel sensor: in vitro and in vivo results. *J Hand Surg* 2007;32:67–75.
- [39] Dodds SD, Panjabi MM, Slade JF 3rd. Screw fixation of scaphoid fractures: a biomechanical assessment of screw length and screw augmentation. *J Hand Surg* 2006;31:405–13.
- [40] Beadel GP, Ferreira L, Johnson JA, King GJ. Interfragmentary compression across a simulated scaphoid fracture—analysis of 3 screws. *J Hand Surg* 2004;29:273–8.
- [41] Grewal R, Assini J, Sauder D, Ferreira L, Johnson J, Faber K. A comparison of two headless compression screws for operative treatment of scaphoid fractures. *J Orthop Surg Res* 2011;6:27.
- [42] Gardner AW, Yew YT, Neo PY, Lau CC, Tay SC. Interfragmentary compression profile of 4 headless bone screws: an analysis of the compression lost on reinsertion. *J Hand Surg* 2012;37:1845–51.